Experimental and Computational Multiphase Flow
Vol. 6, No. 3, 2024, 242–252
https://doi.org/10.1007/s42757-023-0185-5

Experimental analysis of the influence of ambient temperature for a Loop Heat Pipe based Battery Thermal Management System

Marco Bernagozzi[1] (✉), Anastasios Georgoulas[1], Nicolas Miché[1], Marco Marengo[1,2]

1. Advanced Engineering Centre, University of Brighton, Brighton BN2 4GJ, UK
2. Department of Civil Engineering and Architecture, University of Pavia, Pavia 27100, Italy

Abstract

In Battery Thermal Management System (BTMS), Loop Heat Pipes (LHPs) may act as thermal vectors connecting the bottom of the battery pack with the remote chiller of the EV's HVAC system, whilst graphite sheets allow to achieve satisfactory temperature homogenization of the cell surface, containing the added system weight and thermally isolating one cell to the other. This design was developed aiming to improve on fast charge timings, all-electric range and to reduce costs and complexity. Preliminary studies revealed the potential of this innovative passive BTMS for providing better performance than an active BTMS using a liquid cold plate. Taking a further step in the direction of practical applications, the present work investigates how the proposed innovative BTMS performs in different ambient temperatures by showing the results of several fast charge and heating tests inside an environmental thermal chamber, with temperatures ranging between −20 and 50 °C. The results show that the considered LHP worked in all the tested conditions, and that the heating delay brought by the LHP during heating phase (i.e., final temperature 1.2 °C lower than without the LHP) was surpassed by the temperature reduction during the cooling phases (i.e., 3.2 °C temperature reduction at high temperatures).

Keywords

battery thermal management system (BTMS)
electric vehicle (EV)
loop heat pipe (LHP)
thermal chamber
ambient temperature

Article History

Received: 1 September 2023
Revised: 14 December 2023
Accepted: 29 December 2023

Research Article

1 Introduction

To solve the great challenge of limiting the Earth's global warming, the reduction of Green House Gases (GHG) emissions is of vital importance. This needs to be tackled from various angles, from energy production (Chu and Majumdar, 2012), sustainable agricultural practices (Piñeiro et al., 2020), to improved remanufacturing (Fofou et al., 2021) and recycling of goods (Natarajan et al., 2022). One of the biggest strategies sought to tackle global warming, already in place nowadays, is vehicle electrification (Muratori and Mai, 2021; Chen and Yang, 2022; Yang et al., 2023).

Electric Vehicles (EVs) bring along several challenges, one of them being the thermal management of the batteries. Temperature is in fact a critical aspect for the performance and operative life of the battery pack. Due to the transportation of the Li-ions in the electrolyte being affected by the temperature (Kaliaperumal et al., 2021), together with the occurrence of phenomena such as lithium plating (Tomaszewska et al., 2019), the temperature of the battery cells needs to be maintained in precise bands, to ensure acceptable power output, capacity, and operative life (Gantenbein et al., 2019). It has been reported (Zhang et al., 2022) that the optimum temperature range for Li-ion batteries (for commercial EVs) is between 25 and 40 °C, with both electrical power and capacity losses reported both at higher and lower temperatures. Therefore, current EVs need a properly designed Battery Thermal Management System (BTMS), and to achieve this, different cooling technologies are employed. The maximum temperature targets are 40 °C for optimum performance, 50 °C for acceptable performance (Qin et al., 2019), and 60 °C is set as a safety threshold to prevent the occurrence of disruptive phenomena (Tete et al., 2021) (e.g., thermal runaway). Thermal runaway is an unwanted scenario which onsets when the separator melts at around 130 °C and a short circuit leads to large heat release and eventually to the formation of smoke, fire, and explosion (Feng et al., 2018).

✉ m.bernagozzi3@brighton.ac.uk

Nomenclature

BTMS	battery thermal management system	HVAC	heating and ventilation air conditioning
EV	electric vehicle	LHP	loop heat pipe
GHG	green house gases	LPM	lumped parameter model
GWP	global warming potential	ODP	ozone depletion potential
HFCH	highway–fast charge–highway		

Research in the topic of BTMS for EVs has flourished, with lots of work being done to try to limit such thermal management issues. Currently, only liquid and air convection are the BTMS methods employed by automotive manufacturers, due to an understandable scepticism to adopt novel technologies of unknown reliability. However, a plethora of alternative methods are being investigated, and plenty of excellent reviews on the topic can be found in the current literature (Wang et al., 2016; Ianniciello et al., 2018; Wu et al., 2019; Sharma and Prabhakar, 2021; Bernagozzi et al., 2023; Yu et al., 2023). It is important to highlight at this point that literature is scarce of works systematically investigating the effect of ambient temperature on BTMS. Liang et al. (2018) studied the effect of ambient temperature on a hybrid BTMS made by heat pipe and active liquid cooling, but the temperatures were limited to 15, 25, and 35 °C. This work, investigating a temperature range from −20 to 50 °C, presents a significant data point expansion on current literature.

In a previous work (Bernagozzi et al., 2021a), the authors developed a novel BTMS based on Loop Heat Pipes (LHPs) and graphite sheets, aimed at increasing the all-electric range of the vehicle whilst reducing the cost and the charging time. Furthermore, the authors employed for the first time an innovative heat transfer fluid, 3M® Novec® 649, which features extremely low Ozone Depletion Potential (ODP) and Global Warming Potential (GWP) values, on top of not being toxic nor flammable, reducing in this way the risk posed to human safety as well as the risk of pollution (Bernagozzi et al., 2021c). However, all the above-mentioned results were obtained at ambient temperature (i.e., 20 °C), so they are not representative of applications in countries with hotter or colder climates. In fact, Arizona customers have complained about the range of the Nissan Leaf being cut in half compared to what advertised, due to ambient temperatures around 45 °C (Bernagozzi et al., 2023). On the other hand, still the range of the Nissan Leaf has been reported to be reduced from 220 to 110 miles at ambient temperatures of −10 °C (Arora, 2018).

The aim of the present work is to investigate the operation and performance of the proposed novel BTMS in different ambient temperatures, taking a step further in the direction of practical applications. The goals of this investigation are twofold: (i) to understand if the LHP, being a passive device and activating automatically when the right conditions are met, will activate also during heating phases from low temperatures, and hence removing some of the heat provided to the cells by the heaters; this will delay the heating phase and in this work the authors want to investigate and to quantify this detrimental effect; (ii) to investigate the operation at high temperatures, e.g., activation, maximum cell temperatures. To do so, two different layouts, one with LHP and the other one without LHP, are repeatedly tested inside an environmental chamber, allowing the ambient temperature to range between −20 and 50 °C. The BTMS performance is considered during fast charge cycles, as well as during a bespoke driving cycle including motorway driving and fast charge.

2 Battery thermal management system design

The proposed BTMS design, illustrated in Fig. 1, foresees to place an array of thin, flat plate LHPs at the bottom of the cell modules forming the battery pack, acting as thermal vector transferring the excess heat from the cells to a remote chiller (part of the built-in HVAC circuit of the vehicle). Finally, graphite sheets are sandwiched in between the cells to promote cell iso-thermalisation and prevent heat spreading from one cell to another, due to the characteristic anisotropic thermal conductivity of graphite (average values of 350 W/(m·K) on longitudinal direction and 10 W/(m·K) on transversal direction).

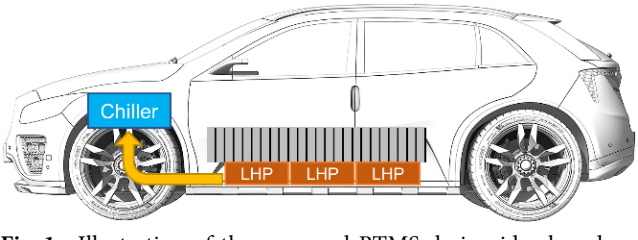

Fig. 1 Illustration of the proposed BTMS design idea based on LHPs. The black lines represent the graphite sheets in between the cells. The size of cells, pack, and LHP are for displaying purposes only and not representative.

LHPs are passive two-phase heat transfer devices, developed in the former Soviet Union in the 1970s, by scientists Gerasimov and Maydanik, for space applications. As standard heat pipes, the heat transfer mechanism relies on perpetual cycles of evaporation and condensation of a working fluid, and they are exceptionally good at removing heat from a source. The uniqueness of LHPs lies in the fact that the characteristic porous structure ("wick"), which ensures the fluid motion due to capillarity, is present in the evaporator only, allowing heat transportation for several meters, at a fraction of the price of standard heat pipes (Maydanik, 2005). LHPs have been successfully used in satellites and aerospace applications for many years (Maydanik, 2005; Su et al., 2019) and have been investigated for ground applications such as electronic cooling (Domiciano et al., 2022), solar collectors (Wang and Yang, 2014).

Figure 2 shows a schematic representation of a flat plate LHP, like the one utilised in this work, to highlight its operation process: firstly, heat is applied to the evaporator by the component that needs cooling and the liquid trapped in the wick then evaporates. Due to capillarity, the generated vapour is then forced to move in one only direction, through the vapour line (which is just a smooth tube) towards the condenser; here, the component is in contact with a cold source, and hence heat is released and condensation occurs; the newly generated liquid travels back to the evaporator along the liquid line (another smooth tube), ending in the compensation chamber, which is a two-phase reservoir that acts as a regulator allowing the operation at different power inputs and temperatures.

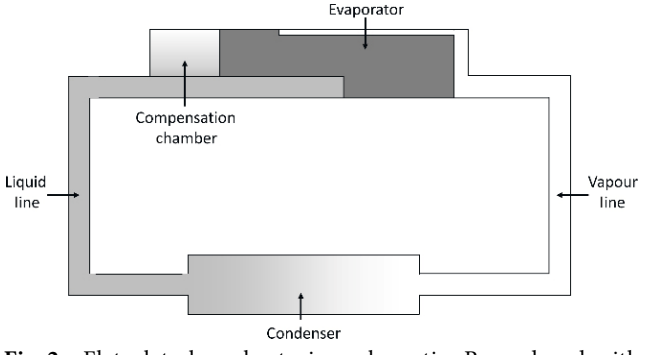

Fig. 2 Flat plate loop heat pipe schematic. Reproduced with permission from Bernagozzi et al. (2021a), © Elsevier Ltd. 2021.

The proposed BTMS, thanks to the use of LHPs (passive devices), provides very effective heat removal and allows to reduce the parasitic power consumption, compared to an active BTMS, therefore allowing for more energy to drive the vehicle and hence increasing its range. The authors already proved that this passive LHP-based BTMS can reduce the cells temperature by more than 3 °C, compared to a standard active liquid cold plate BTMS, during aggressive drive cycles and fast charge rates (Bernagozzi et al., 2021a).

3 Experimental setup

In the experimental setup, for which a schematic diagram is provided in Fig. 3, the battery module is composed of dummy cells, made from 5083-O aluminium plates having the same dimensions as the considered cell type (presented in Table 1 together with the graphite sheets dimensions).

The use of dummy cells is a proven practice already used in literature that allows to minimize the risk of generating excessive thermal stress to a real battery cell, while still evaluating the efficiency of the cooling methods (Karthikeyan et al., 2013; Shah et al., 2016; Liang et al., 2018; Gou and Liu, 2019). The LHP was made from copper and its evaporator was obtained by the Russian company Thercon (https://www.thercon.ru/). Table 2 shows the LHP dimensions.

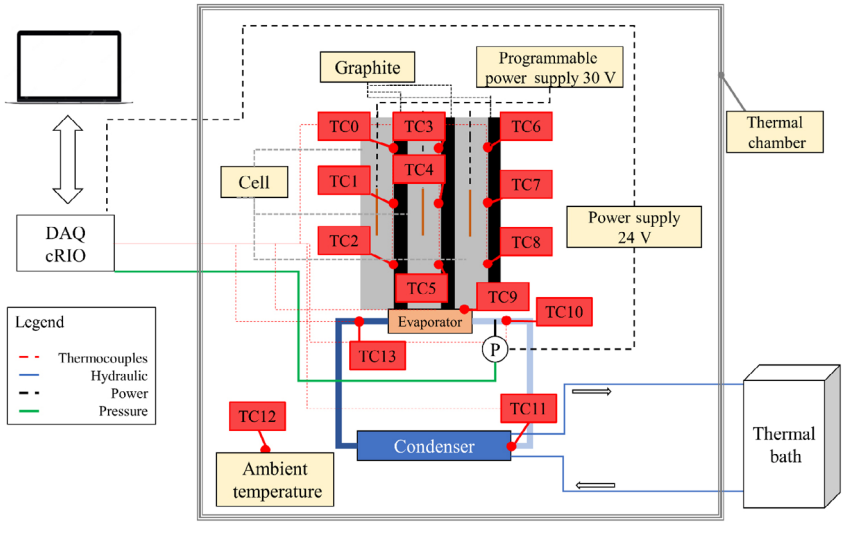

Fig. 3 Experimental set up schematic. *P* is a pressure transducer, measuring the pressure at the exit of the evaporator.

Table 1 Dimension and physical properties of aluminum plates and graphite sheets (RS PRO) used for cell dummy model

Parameter	Aluminium	Graphite	Unit
Thickness	10	0.8	mm
Height	96	96	mm
Width	280	240	mm
Thermal conductivity in-plane, $\lambda_{\parallel}$	109	350	W/(m·K)
Thermal conductivity perpendicular, $\lambda_{\perp}$	109	10	W/(m·K)
Density, ρ	2670	1300–1500	kg/m^3
Specific heat, c_p	900	810	J/(kg·K)

Table 2 LHP dimensions (all parts made in copper)

Part		Value	Unit
Condenser	ID/OD	4.4/6	mm
HEX	ID/OD	15/11	mm
	Length	580	mm
Vapour line	ID/OD	4.4/6	mm
	Length	400	mm
	Elevation	0	cm
Liquid line	ID/OD	4.4/6	mm
	Length	390	mm
	Elevation	0	cm
Wick	Thickness	8	mm
	Width	45	mm
	Length	50.5	mm
	Porosity	45%	
	Pore size	7.3	μm
Vapour grooves	Radius	1.5	mm
	N	9	—
	Length	43	mm
Evaporator shell	Thickness	1	mm
	Width	50	mm
	Length	84	mm
Compensation chamber	Thickness	8	mm
	Width	50.5	mm
	Length	24	mm

The selected working fluid for the LHP was ethanol (filling ratio 60%), chosen due to its low vapour pressure, as pressures greater than 1 bar would have posed mechanical issues to the LHP evaporator's thin copper sheets.

Further details of the equipment used in the setup shown below are given in previous publications by the authors (Bernagozzi et al., 2021a). In the configuration utilised in this work, only the 17% of the bottom of the mock-up battery module is in contact with the active zone of the LHP evaporator, due to fixed geometries of what could be externally sourced, hence representing a limitation to the maximum transmissible heat. However, since the purpose of the experimental demonstrator was to proof the concept of the system and to validate the development of an associated Lumped Parameter Model, which would in turn be used to evaluate the performance of the BTMS, this size discrepancy between LHP evaporator and module footprint was accepted. Similarly, this does not pose a problem in this work, as the conclusions drawn from herein are still valid for larger geometries, i.e., higher contact areas between LHPs and battery module.

The experiments are performed in an environmental chamber (TAS, 4.5 m × 4 m × 3.5 m, Fig. 4) capable of maintain temperatures from −40 to 60 °C with 4 kW of internal load. The tests are performed in a temperature range from −20 to 50 °C, to respect the limits imposed by the operative temperature range set by some of the data acquisition instrumentation.

This work is divided in two experimental campaigns: the first one at temperatures lower than 20 °C and the second one at higher temperatures. In the first part, the effect of the presence of the LHP during heating from lower temperatures is investigated, with particular interest on establishing and quantifying the detrimental effect the LHP has on the heating speed and power required to maintain the battery module to 20 °C. To do so, tests are repeated heating up the battery module with 100 W for 15 min, with and without the presence of the LHP at its bottom. The second part investigates the cooling effect of the LHP-based BTMS at high ambient temperatures, during two different driving cycles, to investigate how much its performances are affected by environmental conditions. The powers are detailed in Fig. 5. Table 3 summarises the list of performed tests.

Fig. 4 TAS environmental chamber used for the tests presented in this work.

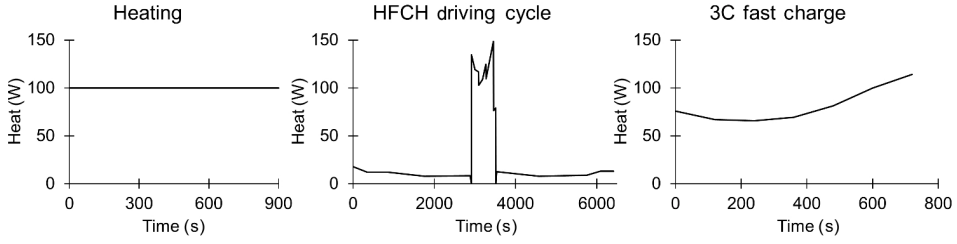

Fig. 5 Heating powers and durations of the different steps of the investigation: left – heating tests, centre – driving cycle tests, right – 3C fast charge.

Table 3 Experimental test summary

#	Chamber temperature T_{amb} (°C)	Heating condition	LHP presence	
1	−20	100 W	Yes	Heating
2			No	
3	−10		Yes	
4			No	
5	0		Yes	
6			No	
7	10		Yes	
8			No	
9	20	HFCH	Yes	Cooling
10		3C	Yes	
11	30	HFCH	Yes	
12		3C	Yes	
13	40	HFCH	Yes	
14		3C	Yes	
15	50	HFCH	Yes	
16		3C	Yes	

The setting up procedure for every test was the same: the thermal chamber was set at the selected ambient temperature and the system was monitored until both the 3-cell module and the LHP reached equilibrium conditions with the ambient. Only then, the heaters were switched on and the data recording started. In other words, in every test the starting temperature of the system was equal to the set ambient temperature.

4 Results

4.1 Heating test results

Figure 6 shows the setup equipped with a heater posed on top of the cell. The heater was composed by an aluminium block with two cartridges inserts (Rotfil® heating cartridge 36 V, 120 W, 6.5 mm × 100 mm). The decision of placing the heating element at the top of the 3-cell module was taken to not move the LHP from the bottom of the module, as main part of the investigation was not to evaluate the

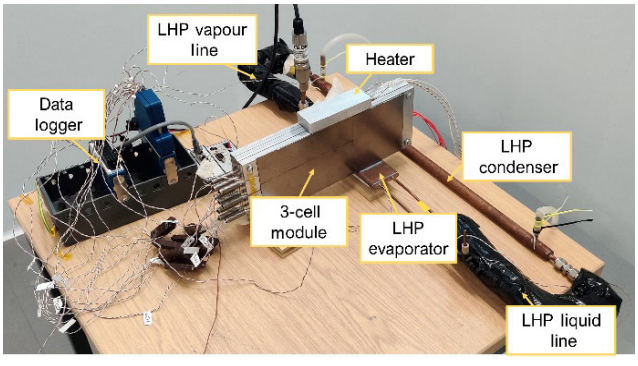

Fig. 6 Setup prepared for the heating tests. Aluminum heater with embedded cartridges placed on top of the 3-cell module.

efficiency of this heating configuration, but to evaluate if the presence of the LHP would have an effect and ultimately quantify it. Moreover, this leaves the door open to evaluate this design by performing numerical simulations in which the bottom surface of the cell module is covered by more LHPs (Bernagozzi et al., 2021b), which will be the next step of this investigation.

It was chosen to supply 100 W heating power to the cells, for a duration of 15 min, as this would make the module average temperature reach optimum temperature from 0 °C (i.e., > 25 °C).

Figure 7 depicts the results of the heating tests with the presence of the LHP (for the ones without the LHP, the results are summarised in Table 4 and Fig. 8, as the trends were not deemed of relevance). One can see how the LHP starts in each instance, as shown by the sudden increase in the vapour line temperature (TC10), proving that hotter vapour is suddenly circulating through the loop, albeit slowly (like in the cases (a) and (b)). Figure 7 shows however that at lower temperatures the LHP start-up takes longer than at higher temperatures.

Comparing the results at the end of the heating phase with and without the presence of the LHP, Table 4 present the final results of the cells temperature (average of the three thermocouples for each cell), together with the cell average temperature $\overline{T}$, which is in turn depicted in Fig. 8 for clarity. It is evident that there is indeed an effect of the LHP in slowing the heating process, by leading to a lower

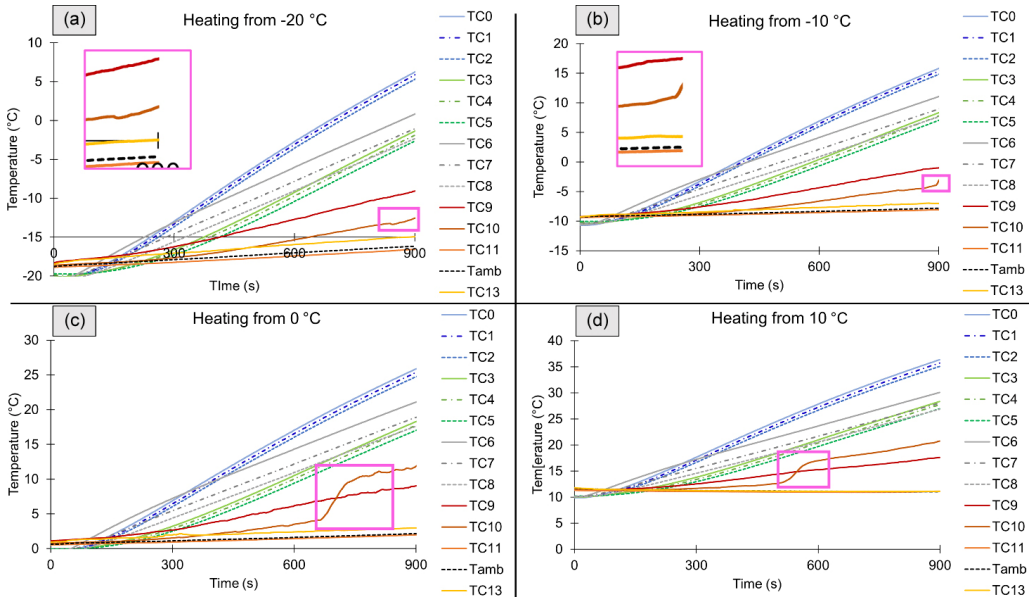

Fig. 7 Results from the heating experiments from −20 °C (a), −10 °C (b), 0 °C (c), and 10 °C (d). These graphs display the temperature trends over a 15 min period 100 W heating phase. The pink boxes and zooms highlight the moment of start-up identification. Reference of the thermocouples positioning can be found in Fig. 3.

Table 4 Result summary of heating tests at low ambient and starting temperature. All temperatures are expressed in °C. $\overline{T}$ stands for average temperature

LHP	T_{amb}	T_{cell1}	T_{cell2}	T_{cell3}	$\overline{T}$
Yes		5.5	−2.2	−1.1	0.7
No	−20	6.1	-0.8	0.1	1.8
Δ		0.6	1.4	1.2	1.1
Yes		15.0	7.4	9.0	10.5
No	−10	15.9	9.0	9.9	11.6
Δ		0.8	1.6	1.0	1.1
Yes		25.0	17.4	19.0	20.5
No	0	25.6	18.9	19.9	21.5
Δ		0.6	1.5	0.9	1.0
Yes		35.5	27.4	28.1	30.3
No	10	36.1	29.5	30.3	32.0
Δ		0.6	2.1	2.2	1.6

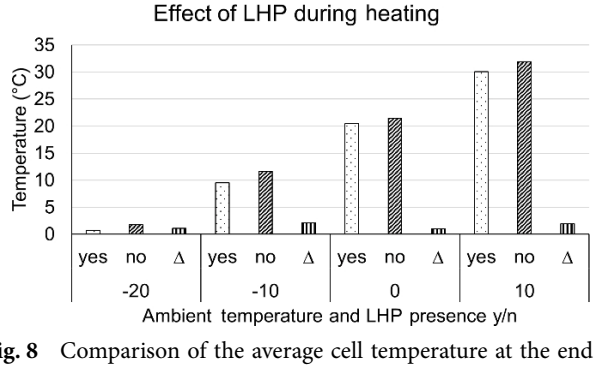

Fig. 8 Comparison of the average cell temperature at the end of the heating phase when the LHP is applied to the battery module and when it is not applied.

temperature at the end of the 15 min. However, data from Table 4 and Fig. 8 indicate that this ΔT does not depend on the ambient temperature, and that it is contained, ranging from 1 to 1.6 °C, averaging to 1.2 °C. This is because the LHP underwent successful start-up even at low temperatures.

4.2 Cooling test results

4.2.1 Driving cycle tests

The driving cycle considered in these experiments comprised of three sections: a 1C① discharge phase (representing fast highway driving), fast charge from 0.2 to 0.8 SOC② in 10 min, and a final section at 1C discharge. This will be herein referred to as HFCH (Highway–Fast Charge–Highway) driving cycle. During the fast charge phase, the maximum charge rate was 4C, which is higher than the state-of-the-art value 3C set by the Porsche Taycan (Tomaszewska et al., 2019). The considered driving cycle was chosen to foresee future developments in the fast charge section, which will allow the technology to provide a sub-10-min charge, being this the target set by industry (Kim et al., 2022).

The heat power released by the cells are mimicked by thin polyimide flexible heaters inserted in between the

① 1C-rate is a measure of how quickly a battery is charged or discharged, and it is defined as the operating current divided the capacity, e.g., 1C means full charge in 1 h, 2C in half an hour and so on.

② SOC is the state of charge, which is a function of the rated capacity and the utilization patterns, denoting the capacity currently available, e.g., SOC1 means battery full and SOC0 means battery dead.

aluminium plates, which in turn are controlled by a programmable power supply that can replicate the trends of the heat released by the cells (as shown in Fig. 3).

Figure 9 presents the temperature (of both cells and LHPs) results of the experimental tests where the BTMS was subjected to the HFCH driving cycle, at different ambient temperatures, from 10 to 50 °C. As highlighted by the dashed line T_{amb}, the ambient temperature underwent some variations during the tests, due to heat transfer from the chamber to the environment, exception made for the cases at 20 and 30 °C, where the small difference with the outside temperature helped maintain the ambient temperature steady. Nevertheless, due to the good insulation of the chamber, the change is limited and never overcomes a ΔT of 5 °C in the almost two-hour long tests, and hence this was deemed acceptable for these tests.

The suddenly upwards trends of vapour line and condenser inlet (TC10 and TC11 respectively), reveal that the LHP started in each test for a wide range of ambient temperatures. In fact, the sudden increase in temperature that the thermocouples record is due to the hot vapour passing through, to indicate that the boiling process and fluid circulation have taken place.

Figure 9 also shows interesting features of the LHP behaviour, as proof of appropriate functioning, such as the decrease of the compensation chamber temperature in the 30 °C, 40 °C, 50 °C cases (TC13 yellow line), to signify the return of the cold condensed liquid to the evaporator. Moreover, shortly after the 100 min mark, the LHP encounters shuts down, with a sudden decrease of the temperature in the vapour line (TC11), meaning that hot vapour is circulating in the loop no more. The fact that the BTMS is showing reproducible analogue behaviour at the different ambient temperature tests is a positive result of this work, going towards a reliable implementation of this BTMS design.

Regarding the start-up process and how this is influenced by the ambient and starting temperature, the graph in Fig. 10 shows that interestingly there is a trend between the time needed for the start-up to take place and the ambient temperature, when subjected to the same power.

Nonetheless, it is interesting to note that these results seem to suggest that the system will be more reactive at higher temperatures, which is to be expected from looking at the graph of dP/dT presented in Fig. 11. Having high values of dP/dT at saturation conditions means that a small change in temperature generates a large change in fluid pressure, augmenting the pumping capability of the bubbles and the whole boiling process (Khandekar et al., 2003; Maydanik, 2005). The authors are aware that this is simply

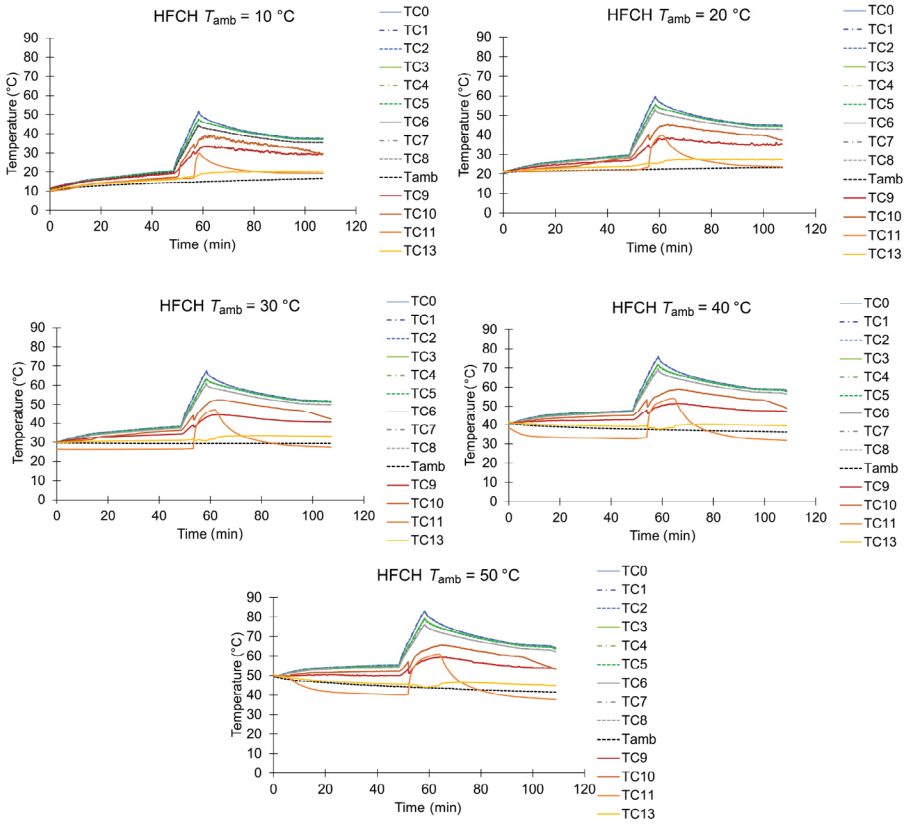

Fig. 9 Test results of BTMS undergoing the HFCH driving cycle at different ambient temperatures, from 10 to 50 °C. For the positioning of the different thermocouples please refer to Fig. 3.

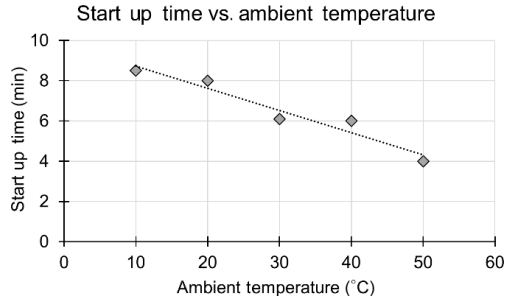

Fig. 10 LHP start-up time at different ambient temperatures.

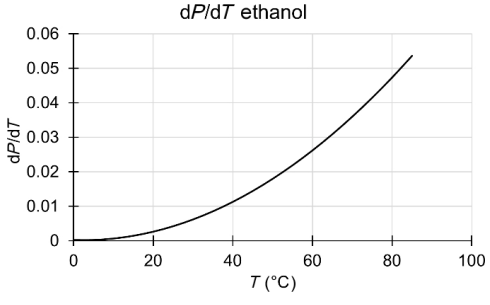

Fig. 11 Trend of the derivative of the pressure over temperature $(\mathrm{d}P/\mathrm{d}T)$ at saturation conditions for ethanol.

a preliminary qualitative case and to draw meaningful conclusions, a more comprehensive testing campaign is needed, perhaps with the heat source directly applied to the LHP evaporator (hence without the cells).

Table 5 sums up the results of the HFCH tests at different ambient temperatures. The temperatures T_{cell1}, T_{cell2}, T_{cell3} are the average of the three thermocouples for the three cells, respectively. Last column also shows that the difference between the maximum temperature and the ambient temperature decreases with the increase of the ambient temperature.

In all cases it is evident from Table 5 that one LHP is not enough to maintain the cells temperature below the optimum values of 40 °C. However, it is already enough to keep them below the acceptable and safety thresholds of 50 and 60 °C in the two first cases, respectively.

4.2.2 Fast charge at 3C test results

To appreciate the effect of the single LHP on the battery module temperature evolution during a 3C test, 8 tests were performed at 4 different temperatures (20, 30, 40, 50 °C) with and without the LHP presence. A 3C fast charge will bring the battery SOC from 20% to 80% in 12 min, with a maximum heat release of 38 W per cell. Results are shown in Table 6 and visually in Fig. 12.

Looking at the temperature reduction that the LHP brings compared to the free convection, one can notice how this Δ value increases with the increase of the ambient temperature.

Table 5 HFCH driving cycle tests at different ambient temperatures. All temperatures are expressed in °C. $\overline{T}$ is the average module temperature and ΔT is the difference between the $\overline{T}$ and T_{amb}

T_{amb}	T_{cell1}	T_{cell2}	T_{cell2}	$\overline{T}$	ΔT
10	51.2	47.6	44.6	47.8	37.8
20	59.4	55.5	52.7	55.9	35.9
30	67.4	63.5	60.7	63.9	33.9
40	75.8	71.8	69.1	72.3	32.3
50	83.2	79.2	76.3	79.6	29.6

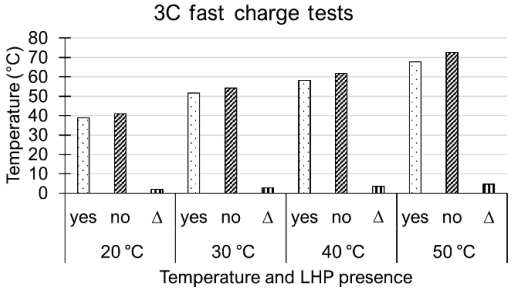

Fig. 12 Results of the 3C fast charge tests, in which the battery module's average temperature is compared between cases with or without the LHP, and the relative difference is highlighted.

Table 6 Results from the 3C fast charge tests at high temperatures. The table shows the cell maximum temperatures after fast charge. All temperatures are expressed in °C. $\overline{T}$ stands for average temperature

LHP	T_{amb}	T_{cell1}	T_{cell2}	T_{cell3}	$\overline{T}$
Yes		40.7	39.2	37.1	39.0
No	20	42.9	41.2	39.0	41.0
Δ		2.2	2.1	1.9	2.0
Yes		53.6	51.7	49.3	51.5
No	30	56.6	54.2	52.1	54.3
Δ		3.0	2.5	2.8	2.7
Yes		60.0	58.3	56.2	58.2
No	40	63.7	61.8	59.5	61.7
Δ		3.7	3.6	3.2	3.5
Yes		69.7	67.9	65.8	67.8
No	50	74.7	72.6	70.2	72.5
Δ		4.9	4.8	4.4	4.7

5 Discussion

The first aim of the investigation outlined in this paper was to understand if the LHP-BTMS would activate at every ambient temperature tested, and despite the non-optimal temperatures reached by the cells during the different experiments at high ambient temperatures, the LHP demonstrated to be able to activate and work in all conditions. It was already known from previous works by the authors

that this specific evaporator design is not the best suited for the considered battery module geometry. However, it was proven that increasing the size of the evaporator (Bernagozzi et al., 2021a) or the number of the evaporators (Bernagozzi et al., 2021b) allowed for exceptional thermal performances (i.e., temperature in optimum range even at high fast charge cycles). This works therefore extends the premise of the LHP application to BTMS, suggesting that this technology can produce good results in a wide range of temperatures, effectively encouraging its adoption in the automotive world.

The second aim was to evaluate the unwanted LHP cooling effect during heating operation. To this extent, Fig. 13 compares the temperature difference between cases with and without the LHP, during both heating and cooling tests. Since the extra unwanted cooling provided by the LHP is not beneficial during the heating phase, for clarity purposes it is reported with a negative sign on the graph (to signify its "negative" effect). In this way, the y axis in Fig. 13 represents ΔT temperature reduction given by the single LHP applied to the 3-cell battery module, compared to when the module is cooled by free convection only. It shows that during heating phases ΔT is not dependant from the ambient temperature, and that the LHP presence worsens the heating process by only 1 °C. On the other hand, during the cooling phase, the LHP does affect the module's temperature incrementally with the ambient temperature, reaching almost 5 °C of difference during the tests at 50 °C. It is also intuitive looking at the red and blue areas in the graph in Fig. 13 that the advantage provided by the LHP-based BTMS during cooling largely outweighs the decrease in performance during heating, which is the significant outcome of this work.

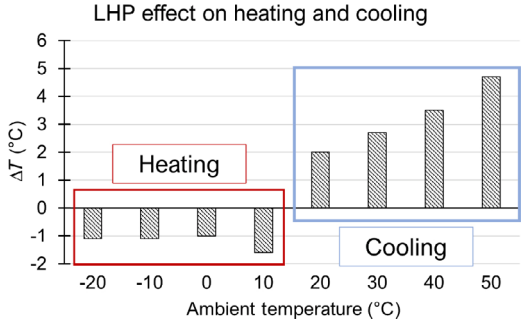

Fig. 13 Effect of the LHP presence on the heating and cooling processes. ΔT value for the heating is represented with a negative sign to signify that it is not a positive outcome.

6 Conclusions

A Battery Thermal Management System (BTMS) using Loop Heat Pipes (LHPs) was investigated at different ambient temperatures, from −20 to 50 °C, thanks to the use of an environmental chamber. The main purpose of this study was to evaluate the effect of the LHP presence during heating and cooling scenarios: firstly, to understand if the BTMS would work at every temperature; secondly, to understand how much the heating phase would be delayed by the presence of the LHP, and if so, how would this handicap compare to the advantages provided by the device during cooling operations at high temperatures. Several tests were repeated with and without the LHP at the bottom of a 3-cell dummy battery module. During the heating tests, 100 W was supplied to the module for 15 min. For the cooling tests, firstly the conditions of a thermally demanding driving cycle with highway driving and fast charge (HFCH) were replicated, and secondly a 3C fast charge cycle was tested. Each condition was tested at different ambient temperatures: −20–10 °C for heating, and 20–50 °C for cooling. The selected working fluid for the utilised copper–copper LHP was ethanol.

The main conclusions that can be drawn from the results are:

(1) LHP start-up took place at each ambient temperature tested; this result advocates for the operational adaptability of the proposed thermal management solution.

(2) During heating from low temperatures (from −10 to 10 °C), the battery module presents a temperature 1.2 °C lower with the presence of the LHP, compared to being heated without the LHP; moreover, this effect seems to be insensitive to the ambient temperature.

(3) During the HFCH driving cycle tests, module temperatures were above the safety threshold of 60 °C when ambient temperature exceeded 30 °C, due to the low heat transfer areas between the two bodies. However, it has been proven by the authors that using an array of parallel LHPs can lead to the desired final temperatures.

(4) A qualitative trend emerged between start-up time and ambient temperature, indicating that start-up takes place quicker at higher temperatures; this suggests that an LHP-based BTMS would be naturally quicker to react at higher temperatures, which is a desirable feature.

(5) Despite the small dimensions of the LHP active zone, the proposed passive BTMS still provided considerable reduction to the maximum average temperature of the module, from 2 to 4.7 °C lower temperatures than free convection only.

(6) Comparing the effect on heating and cooling, the advantage provided by the LHP-based BTMS during cooling clearly outweighs the decrease in performance during heating.

Finally, the results presented herein aim to form the foundation to further evaluate the feasibility of this LHP-based BTMS solution, moving towards an actual industrial application. Future developments of the present study include

the investigation of how a design with more LHPs or a larger active LHP evaporator zone affects the module temperature both at heating and cooling phases. Another next step foresees a further validation of the numerical model already developed by the authors, obtained by matching the results at different ambient temperatures. Following, alternative geometries increasing the heat transfer area between the LHP and the bottom of the battery module will be used in simulations with the same boundary conditions of the tests presented in this work. In fact, the true effect of the LHP presence will be evaluated via numerical simulations, in which the coverage of the module footprint will be increased.

Acknowledgements

The authors would like to thank the Advanced Engineering Centre at the University of Brighton for the financial support.

Declaration of competing interest

The authors have no competing interests to declare that are relevant to the content of this article.

References

Arora, S. 2018. Selection of thermal management system for modular battery packs of electric vehicles: A review of existing and emerging technologies. *Journal of Power Sources*, 400: 621–640.

Bernagozzi, M., Georgoulas, A., Miché, N., Marengo, M. 2023. Heat pipes in battery thermal management systems for electric vehicles: A critical review. *Applied Thermal Engineering*, 219: 119495.

Bernagozzi, M., Georgoulas, A., Miché, N., Rouaud, C., Marengo, M. 2021a. Novel battery thermal management system for electric vehicles with a loop heat pipe and graphite sheet inserts. *Applied Thermal Engineering*, 194: 117061.

Bernagozzi, M., Georgoulas, A., Miché, N., Rouaud, C., Marengo, M. 2021b. Comparison between different battery thermal management systems during fast charge cycles. In: Proceedings of the 17th UK Heat Transfer Conference, 4–6.

Bernagozzi, M., Miché, N., Georgoulas, A., Rouaud, C., Marengo, M. 2021c. Performance of an environmentally friendly alternative fluid in a loop heat pipe-based battery thermal management system. *Energies*, 14: 7738.

Chen, X., Yang, J. 2022. Potential benefit of electric vehicles in counteracting future urban warming: A case study of Hong Kong. *Sustainable Cities and Society*, 87: 104200.

Chu, S., Majumdar, A. 2012. Opportunities and challenges for a sustainable energy future. *Nature*, 488: 294–303.

Domiciano, K. G., Krambeck, L., Flórez, J. P. M., Mantelli, M. B. H. 2022. Thin diffusion bonded flat loop heat pipes for electronics: Fabrication, modelling and testing. *Energy Conversion and Management*, 255: 115329.

Feng, X., Ouyang, M., Liu, X., Lu, L., Xia, Y., He, X. 2018. Thermal runaway mechanism of lithium ion battery for electric vehicles: A review. *Energy Storage Materials*, 10: 246–267.

Fofou, R. F., Jiang, Z., Wang, Y. 2021. A review on the lifecycle strategies enhancing remanufacturing. *Applied Sciences*, 11: 5937.

Gantenbein, S., Schönleber, M., Weiss, M., Ivers-Tiffée, E. 2019. Capacity fade in lithium-ion batteries and cyclic aging over various state-of-charge ranges. *Sustainability*, 11: 6697.

Gou, J., Liu, W. 2019. Feasibility study on a novel 3D vapor chamber used for Li-ion battery thermal management system of electric vehicle. *Applied Thermal Engineering*, 152: 362–369.

Ianniciello, L., Biwolé, P. H., Achard, P. 2018. Electric vehicles batteries thermal management systems employing phase change materials. *Journal of Power Sources*, 378: 383–403.

Kaliaperumal, M., Dharanendrakumar, M. S., Prasanna, S., Abhishek, K. V., Chidambaram, R. K., Adams, S., Zaghib, K., Reddy, M. V. 2021. Cause and mitigation of lithium-ion battery failure—A review. *Materials*, 14: 5676.

Karthikeyan, V. K., Ramachandran, K., Pillai, B. C., Solomon, A. B. 2013. Effect of number of turns on the temperature pulsations and corresponding thermal performance of pulsating heat pipe. *Journal of Enhanced Heat Transfer*, 20: 443–452.

Khandekar, S., Dollinger, N., Groll, M. 2003. Understanding operational regimes of closed loop pulsating heat pipes: An experimental study. *Applied Thermal Engineering*, 23: 707–719.

Kim, S., Tanim, T. R., Dufek, E. J., Scoffield, D., Pennington, T. D., Gering, K. L., Colclasure, A. M., Mai, W., Meintz, A., Bennett, J. 2022. Projecting recent advancements in battery technology to next-generation electric vehicles. *Energy Technology*, 10: 2200303.

Liang, J., Gan, Y., Li, Y. 2018. Investigation on the thermal performance of a battery thermal management system using heat pipe under different ambient temperatures. *Energy Conversion and Management*, 155: 1–9.

Maydanik, Y. F. 2005. Loop heat pipes. *Applied Thermal Engineering*, 25: 635–657.

Muratori, M., Mai, T. 2021. The shape of electrified transportation. *Environmental Research Letters*, 16: 011003.

Natarajan, S., Divya, M. L., Aravindan, V. 2022. Should we recycle the graphite from spent lithium-ion batteries? The untold story of graphite with the importance of recycling. *Journal of Energy Chemistry*, 71: 351–369.

Piñeiro, V., Arias, J., Dürr, J., Elverdin, P., Ibáñez, A. M., Kinengyere, A., Opazo, C. M., Owoo, N., Page, J. R., Prager, S. D., et al. 2020. A scoping review on incentives for adoption of sustainable agricultural practices and their outcomes. *Nature Sustainability*, 3: 809–820.

Qin, P., Liao, M., Zhang, D., Liu, Y., Sun, J., Wang, Q. 2019. Experimental and numerical study on a novel hybrid battery thermal management system integrated forced-air convection and phase change material. *Energy Conversion and Management*, 195: 1371–1381.

Shah, K., McKee, C., Chalise, D., Jain, A. 2016. Experimental and numerical investigation of core cooling of Li-ion cells using heat pipes. *Energy*, 113: 852–860.

Sharma, D. K., Prabhakar, A. 2021. A review on air cooled and air centric hybrid thermal management techniques for Li-ion battery packs in electric vehicles. *Journal of Energy Storage*, 41: 102885.

Su, Q., Chang, S., Song, M., Zhao, Y., Dang, C. 2019. An experimental study on the heat transfer performance of a loop heat pipe system with ethanol–water mixture as working fluid for aircraft anti-icing. *International Journal of Heat and Mass Transfer*, 139: 280–292.

Tete, P. R., Gupta, M. M., Joshi, S. S. 2021. Developments in battery thermal management systems for electric vehicles: A technical review. *Journal of Energy Storage*, 35: 102255.

Tomaszewska, A., Chu, Z., Feng, X., O'Kane, S., Liu, X., Chen, J., Ji, C., Endler, E., Li, R., Liu, L., et al. 2019. Lithium-ion battery fast charging: A review. *eTransportation*, 1: 100011.

Wang, Q., Jiang, B., Li, B., Yan, Y. 2016. A critical review of thermal management models and solutions of lithium-ion batteries for the development of pure electric vehicles. *Renewable and Sustainable Energy Reviews*, 64: 106–128.

Wang, Z., Yang, W. 2014. A review on loop heat pipe for use in solar water heating. *Energy and Buildings*, 79: 143–154.

Wu, W., Wang, S., Wu, W., Chen, K., Hong, S., Lai, Y. 2019. A critical review of battery thermal performance and liquid based battery thermal management. *Energy Conversion and Management*, 182: 262–281.

Yang, A., Liu, C., Yang, D., Lu, C. 2023. Electric vehicle adoption in a mature market: A case study of Norway. *Journal of Transport Geography*, 106: 103489.

Yu, Z., Zhang, J., Pan, W. 2023. A review of battery thermal management systems about heat pipe and phase change materials. *Journal of Energy Storage*, 62: 106827.

Zhang, X., Li, Z., Luo, L., Fan, Y., Du, Z. 2022. A review on thermal management of lithium-ion batteries for electric vehicles. *Energy*, 238: 121652.